New side chain LC polysiloxanes with carbonyl-bound chiral terminal group‡

by MIKHAIL V. KOZLOVSKY*†,
EDUARDO ARTURO SOTO BUSTAMANTE and WOLFGANG HAASE
Institute for Physical Chemistry, Technical University Darmstadt, Darmstadt, Germany

A synthetic route has been developed to a new series of homo- and co-polysiloxanes with a terminal chiral 2-(*S*)-butyl fragment attached to the mesogenic biphenyl core via the ketone binding group, >C=O. The synthesis, structure and ferroelectric properties of the polymers are reported. All the polymers show in their S_A phases an unusual decrease in the interlayer distance with increasing temperature.

1. Introduction

For most ferroelectric smectic C* LC polymers synthesized up to now, a chiral fragment is attached to a mesogenic rigid core by the ether, −O− or ester, −COO−, binding group [1–4]. On the other hand, many other binding or attachment groups have been tested for low molar mass ferroelectric liquid crystals, particularly the ketone group, >C=O, which leads to materials with rather high values of the spontaneous polarization, P_S [5–7]. In the few examples of polymers, [8, 9] containing a chiral 2-methylalkylcarbonyl fragment, this is connected to an isolated benzene ring which is linked in turn to a carboxyl group, which breaks any further π-electron conjugation.

LC polymers with a chiral carbon atom directly attached to a conjugated π-electron system should be of interest for non-linear optical applications, especially if they form ferroelectric smectic C* phases. As a first step towards such structures, we have synthesized a number of homo- and co-polysiloxanes with biphenyl alkyl ketone side groups

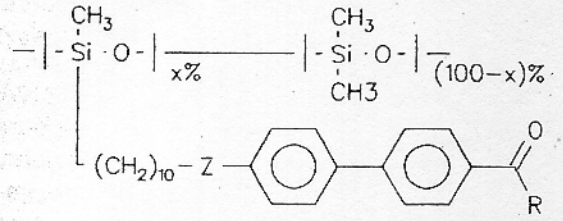

where $Z = -CH_2-O-$ or $-COO-$, $x = 100$ or 33, and $R = -C^*H(CH_3)-C_2H_5$ or $-CH_2-CH(CH_3)_2$.

Here we report the synthesis of the homo- and co-polymers, the results of microscopic, DSC and X-ray structural studies of their mesophases and the ferroelectric properties of the chiral polymers.

2. Experimental

2.1. *Synthetic procedures*

The synthesis of the monomers is based on the scheme suggested by Yoshizawa *et al.* [6] involving acylation of *p*-methoxybiphenyl and subsequent deprotection of the phenolic −OH group

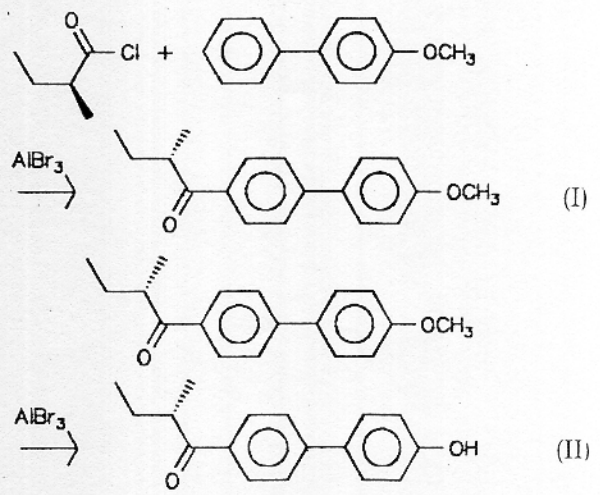

The resulting 4-hydroxy-4′-(2-(*S*)-methylbutyryl)biphenyl was converted into monomers using standard chemical procedures of etherification:

*Author for correspondence.
†Research Fellow from the Institute of Crystallography, Russian Academy of Sciences, Moscow, Russia

‡Presented at the European Conference on Liquid Crystals, Bovec, Slovenia, March 1995.

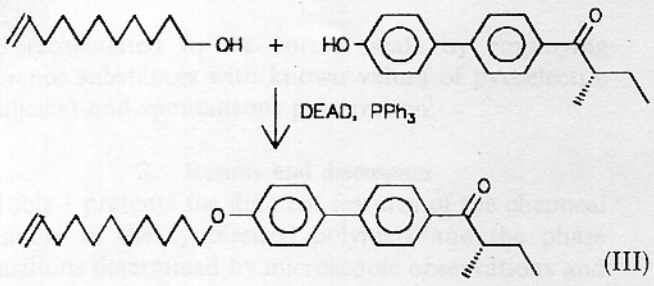

(III)

and esterification:

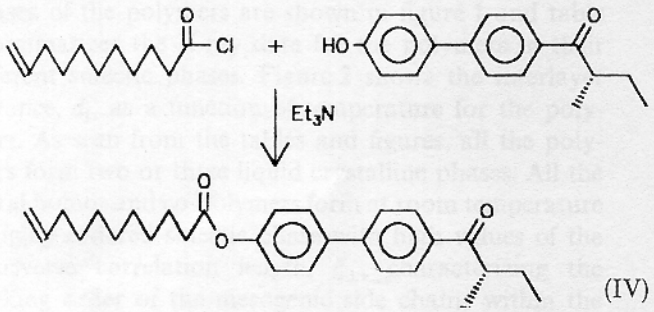

(IV)

2.1.1. *4-Methoxy-4′-(2-(S)-methylbutyryl)biphenyl* (**I**)

The acylation complex prepared by dissolving the aluminium bromide, previously cooled in an ice-water bath, in 2-(*S*)-methylbutyryl chloride, was added dropwise (in 1·2 mol excess) to a suspension of the 4-methoxybiphenyl in dichloromethane at 0°C in a nitrogen atmosphere. Then the reaction mixture was stirred for 2 h at 0°C and overnight at room temperature, before heating for 6 h under reflux and pouring onto ice acidified by HCl. The organic layer was separated, and the water layer extracted twice with dichloromethane. The combined organic layers were dried over $CaCl_2$. The crude product, after evaporation of the solvent, was chromatographed (kieselgel column, toluene–hexane 1 : 1 mixture) giving the ketone (**I**) in about 25% yield. M.p. 114°C, ^{1}H NMR δ ppm ($CDCl_3$): 0·95 (3H, t, $CH_2\underline{CH}_3$), 1·22 (3H, d, C*H$\underline{CH}_3$), 1·55 and 1·85 (2H, m, C*H$\underline{CH}_2$CH$_3$), 3·45 (1H, m, C*H), 3·85 (3H, s, OCH_3), 7·05, 7·70, 7·80 and 8·05 (8H, d, aromatic).

The optically inactive 4-methoxy-4′-(3-methylbutyryl)biphenyl was prepared in the same way using isovaleryl chloride; m.p. 104°C.

2.1.2. *4-Hydroxy-4′-(2-(S)-methylbutyryl)biphenyl* (**II**)

The above ketone (**I**) was stirred with aluminium bromide in dry toluene for 1·5 h at 0°C, overnight at room temperature and for 5 h under reflux. The reaction mixture was poured into ice water and the product extracted with ether. The organic layer was washed by water and dried over $CaCl_2$. Column chromatography on kieselgel using as eluent, first toluene and then a toluene–ethyl acetate 9 : 1 mixture, gave the end product (**II**) in an average yield of 70%. M.p. 137°C. ^{1}H NMR δ ppm ($CDCl_3$): 0·95 (3H, t, $CH_2\underline{CH}_3$), 1·22 (3H, d, C*H$\underline{CH}_3$), 1·55 and 1·85 (2H, m, C*H$\underline{CH}_2$CH$_3$), 3·45 (1H, m, C*H), 5·60 (1H, brs, OH), 7·05, 7·70, 7·80 and 8·05 (8H, d, aromatic).

The optically inactive 4-hydroxy-4′-(3-methylbutyryl)biphenyl was prepared in the same way: m.p. 145°C.

2.1.3. *Preparation of the polymers*

All the polymers were synthesized from the corresponding monomers by the standard polyhydrosilylation procedure using poly(methyl hydrogen siloxane), $M \approx 2100$ (E Merck, Darmstadt, Germany), for the homopolymers, or copoly((30–35%) methyl hydrogen-(65–70%) dimethylsiloxane), with an average molar mass determined from the viscosity correlation as $M \approx 2000$–2100 (ABCR, Karlsruhe, Germany), for the copolymers. The starting polysiloxane and a 10 mol % excess of the appropriate monomer **III** or **IV** (with respect to Si–H bonds) were dissolved in dry toluene and heated to 100–105°C under nitrogen. Then a freshly prepared solution of chloroplatinic acid, H_2PtCl_6, in isopropanol (0·1 g ml^{-1}) was added to give a Pt/alkene ratio about 5×10^{-4}. The mixture was stirred for 72 h at the same temperature under N_2. Then the polymers were reprecipitated 7–10 times from dichloromethane using methanol. ^{1}H NMR confirmed the complete convertion (absence of Si–H protons).

2.2. *Investigation techniques*

DSC curves were recorded using a Perkin-Elmer DSC-2C calorimeter. Microscopic textures and optical switching were observed using 10 μm cells (EHC, Japan) and a Leitz microscope equipped with a Mettler FP-82 heating stage and a Panasonic AG-7330 video recording system. X-ray scattering curves were measured by a STOE-2 diffractometer using CuK_α radiation and a PSD linear position scanning detector.

The interlayer distance, d_1, and the spacing of the mesogenic side chains within the smectic layer, D, were calculated from the positions of the first order small angle X-ray peak and the wide angle scattering peaks, respectively. The related correlation lengths, $\xi_\parallel$ and $\xi_\perp$, were calculated from $\xi = \lambda/\pi\Delta(2\theta)$, where $\lambda = 1{\cdot}54$ Å is the wavelength of the X-ray radiation and $\Delta(2\theta)$ is the width at half maximum of the corresponding X-ray peak.

The pyroelectric effect was studied by a laboratory-made set-up. A laser diode operating at 686 nm with a light power of 30 mW produced the temperature increment in the electro-optic cell under an applied bias d.c. voltage of 70 V. The intensity of the laser emission was modulated by a function generator (70Hz). The pyroelectric response was measured as a sine voltage across the load resistor R = 10 MΩ using a lock-in amplifier

and recalculated to the correct scale by employing reference substances with known values of pyroelectric coefficient and spontaneous polarization.

3. Results and discussion

Table 1 presents the different features of the chemical structure of the synthesized polymers and the phase transitions determined by microscopic observations and X-ray studies, supported by the DSC measurements. Typical X-ray diffraction curves for the different smectic phases of the polymers are shown in figure 1 and table 2 summarizes the X-ray data for the polymers in their different smectic phases. Figure 2 shows the interlayer distance, d_1, as a function of temperature for the polymers. As seen from the tables and figures, all the polymers form two or three liquid crystalline phases. All the chiral homo- and co-polymers form at room temperature a highly ordered smectic phase with high values of the transverse correlation length, $\xi_\perp$, characterizing the packing order of the mesogenic side chains within the smectic layer. Moreover, for the polymers PS-1 and CPS-1, this phase shows two wide angle X-ray diffraction peaks, which are characteristic for orthorombic and monoclinic crystal smectic phases (figure 1 (*e*)). The conclusion about the tilted H* phase structure has been reached from the interlayer distance compared with the corresponding value for the higher temperature S_A phase (table 2, figure 2). For the copolymer CPS-1, the ferroelectric nature of the phase has been confirmed by pyroelectric measurements (see below). The homopolymer PS-2 forms the less ordered tilted S_F^* phase, but the corresponding 'diluted' copolymer CPS-2 gives an orthogonal S_B phase, both having a single sharp wide angle reflection (figures 1 (*c*) and (*d*)). On the other hand, the non-chiral model polymer PS-0 forms, at room temperature, a disordered tilted S_C phase (figure 1 (*b*)). The X-ray pattern of an oriented film of the copolymer CPS-2 is also characteristic of a S_B phase, showing sharp equatorial arcs at wide angles, with two pairs of meridional small angle crescents.

The high temperature S_A mesophases of all the polymers studied show similar X-ray scattering curves with two orders of small angle diffraction peaks, as shown in figure 1 (*a*). As seen from figure 2, the 'diluting' of the polymer main chain results in drastic changes in the d_1 values from a monolayer packing for the homopolymers, $d_1 \approx 33$–34 Å (compare with the calculated length of the side chain, $l \approx 29{\cdot}3$ Å), to a bilayer packing with mutual penetration of the mesogenic groups of neighbouring layers, $d_1 \approx 41$–47 Å. This fact is supported by the chemical nature of the copolymers, having one third only of the monomer units carrying mesogenic moieties, so that a large amount of empty space between these groups enables overlapping of the layers.

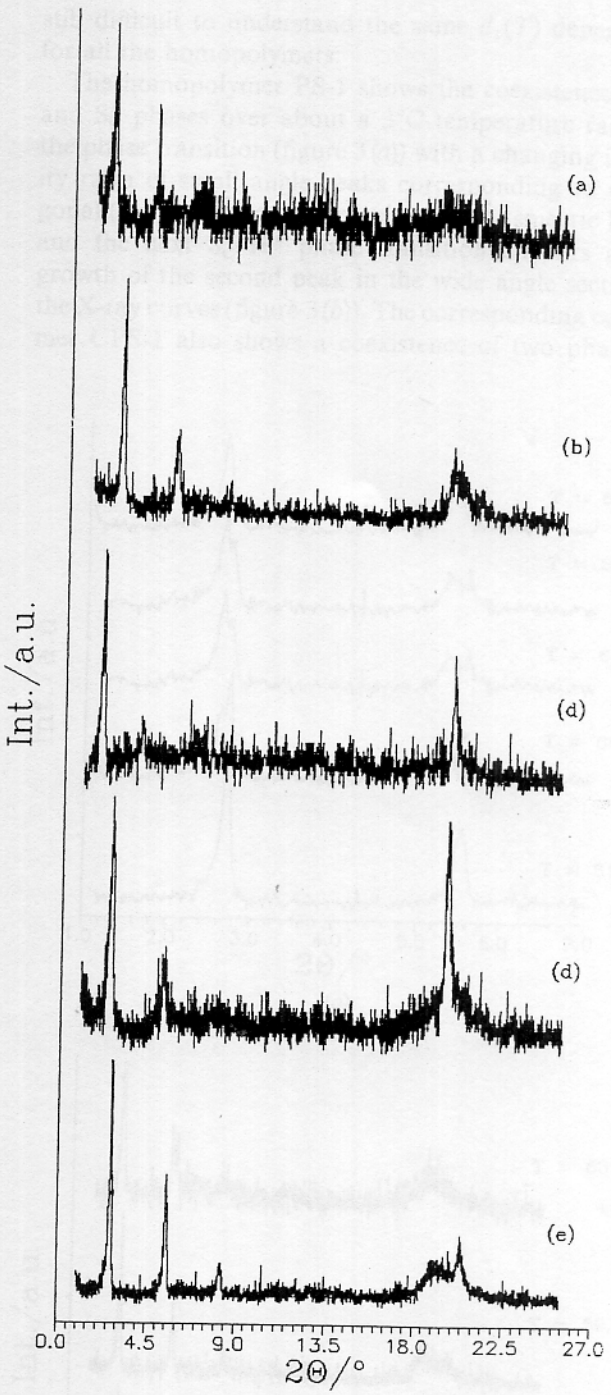

Figure 1. Typical X-ray diffraction curves for the polymers: (*a*) S_A phase (CPS-1, 58·5°C); (*b*) S_C phase (PS-0, 113°C). (*c*) S_B phase (CPS-2, 18·5°C), (*d*) S_F^* phase (PS-2, 43°C). and (*e*) H* phase (PS-1, 30°C).

All the homo- and copolymers show a decrease of the interlayer distance in the S_A phase with increasing temperature, the opposite trend to that for the S_C phase and quite an unusual behaviour for a S_A phase. The effect is most pronounced for CPS-2, as the decrease in the d_1

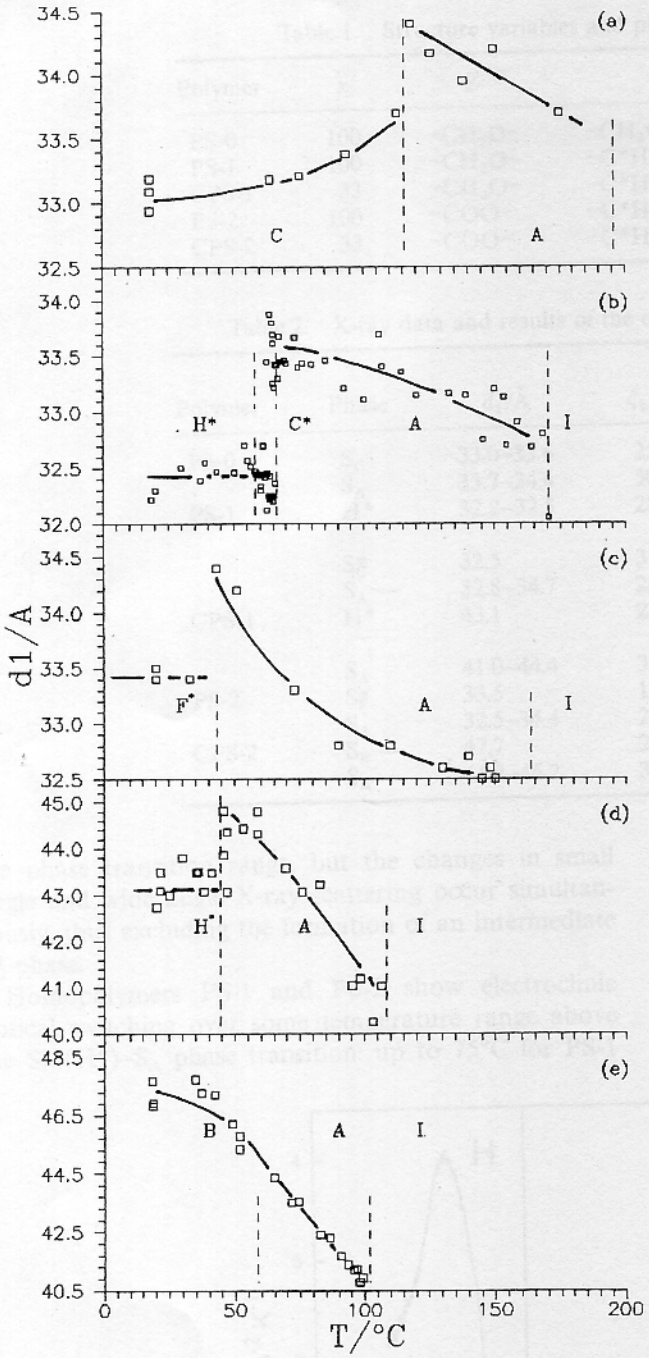

Figure 2. Interlayer distance, d_1, versus temperature for the different smectic phases (A, C etc) and the H* phase of the polymers PS-0 (*a*), PS-1 (*b*), PS-2 (*c*), CPS-1 (*d*), and CPS-2 (*e*).

value amounts to about 7·5 Å, or about 20 per cent of the total value. Such a behaviour could be explained for the copolymers as a result of decreased viscosity and the increased mobility of the spacers and main chains that enables deeper overlap of the layers, nevertheless, it is still difficult to understand the same $d_1(T)$ dependence for all the homopolymers.

The homopolymer PS-1 shows the coexistence of S_A and S_C^* phases over about a 3°C temperature range at the phase transition (figure 3 (*a*)) with a changing intensity ratio of small angle peaks corresponding to orthogonal ($d_1 \approx 33{\cdot}6$ Å) and tilted ($d_1 \approx 32{\cdot}4$ Å) smectic layers, and the next S_C^*–H* phase transition appears as the growth of the second peak in the wide angle section of the X-ray curves (figure 3 (*b*)). The corresponding copolymer CPS-1 also shows a coexistence of two phases in

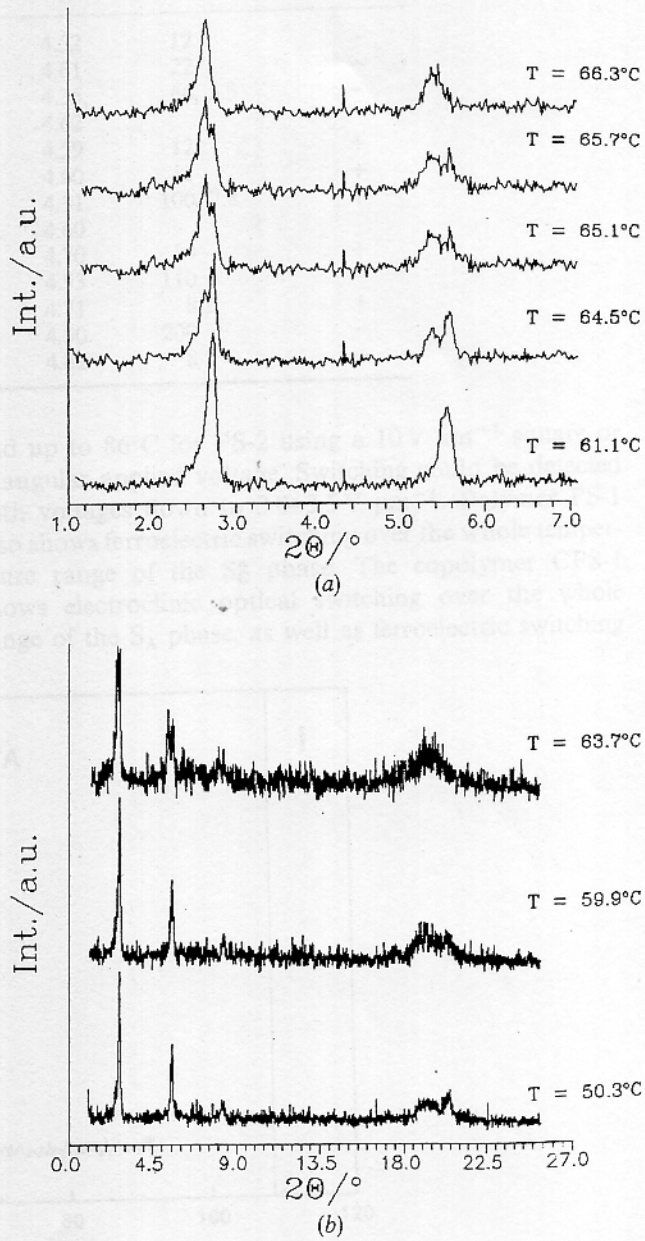

Figure 3. The S_C^*–S_A (*a*) and H*–S_C^* (*b*) phase transitions of the polymer PS-1 as observed by X-ray scattering.

Table 1. Structure variables and phase transitions of the polymers.

Polymer	x	Z	R	Phase transitions
PS-0	100	$-CH_2O-$	$-CH_2CH(CH_3)_2$	S_C 115 S_A 196 I
PS-1	100	$-CH_2O-$	$-C^*H(CH_3)-C_2H_5$	H*58 S_C^* 66 S_A 170 I
CPS-1	33	$-CH_2O-$	$-C^*H(CH_3)-C_2H_5$	H* 45 S_A 99 I
PS-2	100	$-COO-$	$-C^*H(CH_3)C_2H_5$	S_F^* 44 S_A 164 I
CPS-2	33	$-COO-$	$-C^*H(CH_3)C_2H_5$	S_B 59 S_A 102 I

Table 2. X-ray data and results of the optical switching test for the polymers.

Polymer	Phase	d_1/Å	$\xi_\parallel$/Å	D/Å	$\xi_\perp$/Å	Optical switching
PS-0	S_C	33.0–33.6	250	4.52	12	–
	S_A	33.7–34.4	500	4.61	22	–
PS-1	H*	32.2–32.5	280	4.35, 4.62	66, 5.5	–
	S_C^*	32.5	310	4.59	12	+
	S_A	32.8–34.7	280	4.60	11	+
CPS-1	H*	43.1	280	4.31, 4.60	100, 7.8	+
	S_A	41.0–44.4	330	4.70	14	+
PS-2	S_F^*	33.5	170	4.53	110	–
	S_A	32.5–34.4	270	4.71	8.2	+
CPS-2	S_B	47.7	210	4.50	200	–
	S_A	41.2–46.2	360	4.62	8	–

the phase transition range, but the changes in small angle and wide angle X-ray scattering occur simultaneously, thus excluding the formation of an intermediate S_C^* phase.

Homopolymers PS-1 and PS-2 show electroclinic optical switching over some temperature range above the S_C^* (H*)–S_A phase transition: up to 75°C for PS-1 and up to 86°C for PS-2 using a 10 V μm^{-1} square or triangular applied voltage. Switching could be detected with voltages down to 3·0–3·5 V μm^{-1}. Polymer PS-1 also shows ferroelectric switching over the whole temperature range of the S_C^* phase. The copolymer CPS-1 shows electroclinic optical switching over the whole range of the S_A phase, as well as ferroelectric switching

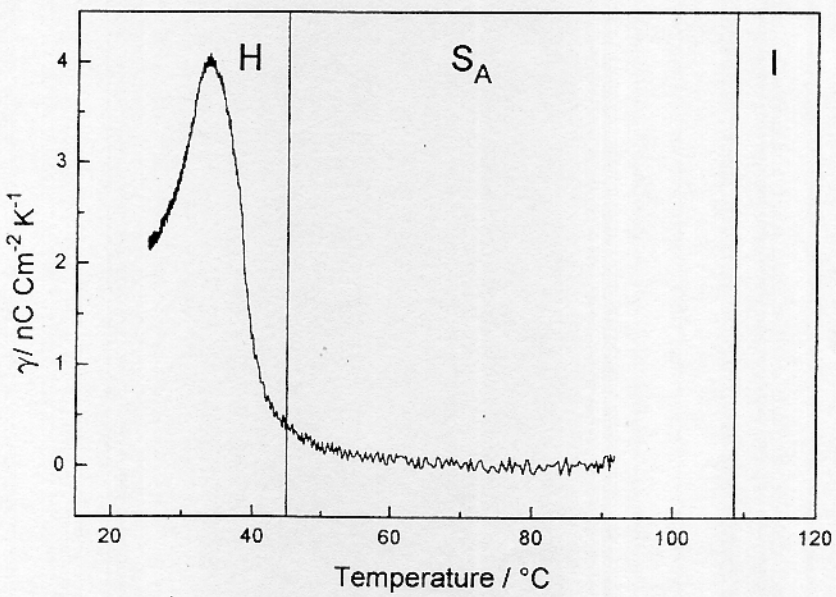

Figure 4. The pyroelectric response from the copolymer CPS-1 versus temperature in terms of the apparent pyroelectric coefficent, γ.

in the H* phase down to 31·5°C (at 10 V μm^{-1}); this can be related to the increased mobility of the main chain, and therefore, at the macroscopic level, to the lower viscosity of the copolymer as compared with the corresponding homopolymer. The same factor, however, results in a very pronounced electrohydrodynamic instability in the cell, which can be observed starting from about 68°C. Figure 4 shows the pyroelectric response, γ, of the copolymer CPS-1 versus temperature for an applied bias voltage of 4 V μm^{-1}. The sharp nature of the curve is typical for ferroelectric LC polymers, thus confirming the tilted chiral structure of the low temperature phase, although the voltage applied is certainly insufficient to obtain saturation of the effect and, therefore, calculation of the value of the spontaneous polarization for the copolymer.

4. Conclusion

These polysiloxanes with a chiral terminal group attached to an aromatic mesogenic core could be promising as materials with a broad range of electroclinic switching in the S_A phase. The detailed structure of the S_A phase and the nature of its unusual temperature dependence of smectic layer thickness require further investigation.

We are grateful to Dr B. Ostrovskii (Institute of Crystallography, Moscow, Russia) for valuable discussions. The work has been personally supported (M. V. Kozlovsky) by the Alexander von Humboldt Foundation, Germany)

References

[1] Le Barny, P., and Dubois, J. C., 1989, in: *Side Chain Liquid Crystal Polymers*, edited by C.B. McArdle, (Glasgow: Blackie), pp. 130–158.

[2] Kozlovsky, M. V., and Beresnev, L. A., 1992, *Phase Transitions*, **40**, 129.

[3] Sherowsky, G., 1993, *Makromol. Chem., Macromol. Symp.*, **69**, 87.

[4] Chiellini, E., Galli, G., Cioni, F., and Dossi, E., 1993, *Makromol. Chem., Macromol. Symp.*, **69**, 51.

[5] Kobayashi, S., and Ishibashi, S., 1992, *Mol. Cryst. liq. Cryst.*, **220**, 1.

[6] Yoshizawa, A., Yokoyama, A., and Nishiyama, I., 1992, *Liq. Cryst.*, **11**, 235.

[7] Sakaigawa, A., Tashiro, Y., Aoki, Y., and Nohira, H., 1991, *Mol. Cryst. liq. Cryst.*, **206**, 147.

[8] Takahashi, K., Ishibashi, S., and Yamamoto, F., 1993, *Ferroelectrics*, **148**, 715.

[9] Ishibashi, S., Takahashi, K., Ishizawa, S., and Yamamoto, F., 1993, *Ferroelectrics*, **148**, 737.